Biophysical Journal, Volume *110*

Supplemental Information

A pH-Mediated Topological Switch within the N-Terminal Domain of Human Caveolin-3

Ji-Hun Kim, Jonathan P. Schlebach, Zhenwei Lu, Dungeng Peng, Kaitlyn C. Reasoner, and Charles R. Sanders

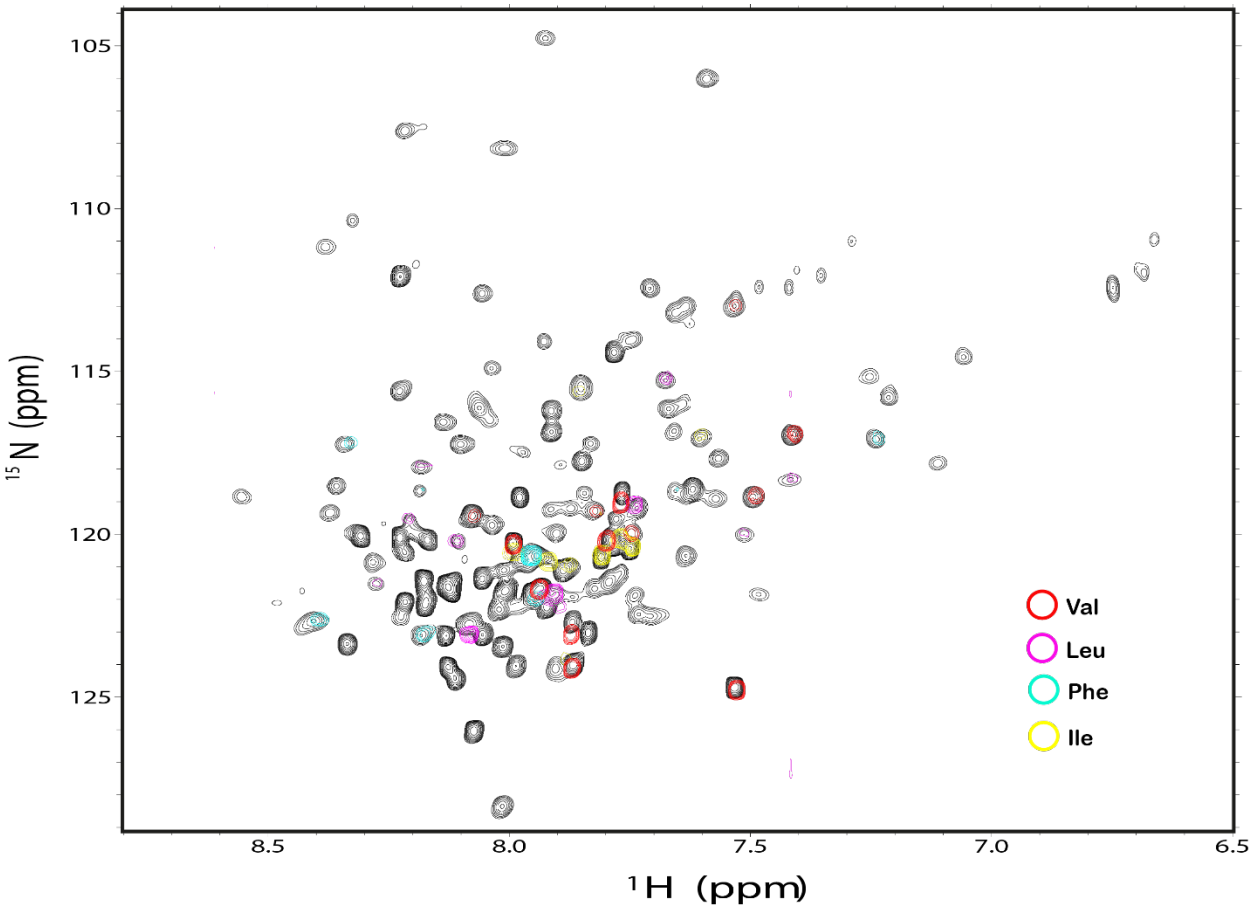

Figure S1. Selective ^{15}N amino acid labeling of lipidated Cav3 in LPPG micelles. The ^{1}H ^{15}N TROSY-HSQC spectra of isotopically labeled lipidated Cav3 in LPPG micelles at pH 6.5 and 45°C are shown. Spectra of lipidated Cav3 bearing isotopically labeled ^{15}N-Val (red), ^{15}N-Leu (pink), ^{15}N-Phe (cyan), ^{15}N-Ile (yellow) are superimposed on the spectrum for the uniformly ^{15}N-labeled lipidated Cav3 (black). These data were used to help complete assignments for the TROSY-HSQC resonances.

Figure S2
Kim et al.

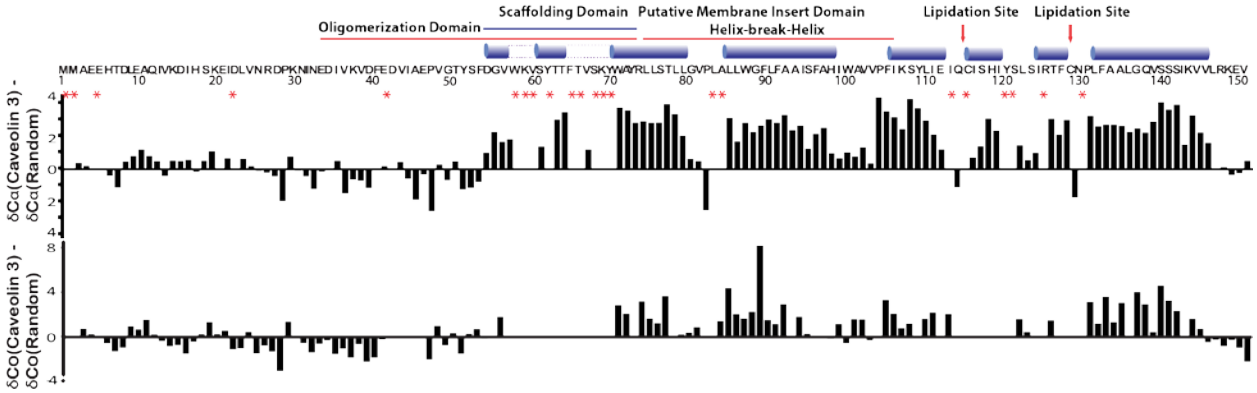

Figure S2. Secondary structure of lipidated Cav3 in LPPG micelles. Secondary structure predictions based on Chemical Shift Index (CSI, top) are shown for lipidated Cav3. The differences between the observed ^{13}C chemical shifts and standard residue-specific random coil ^{13}C shift values for the backbone carbons (ΔC) are plotted against the residue number. According to CSI analysis consecutive positive ΔC values in $^{13}C\alpha$ and ^{13}CO are indicative of α helical secondary structure. TalosN-based analysis of these same chemical shifts, which are summarized above the annotated sequence, are generally consistent with the results of CSI. Red asterisks mark residues that could not be confidently assigned.

Figure S3
Kim et al.

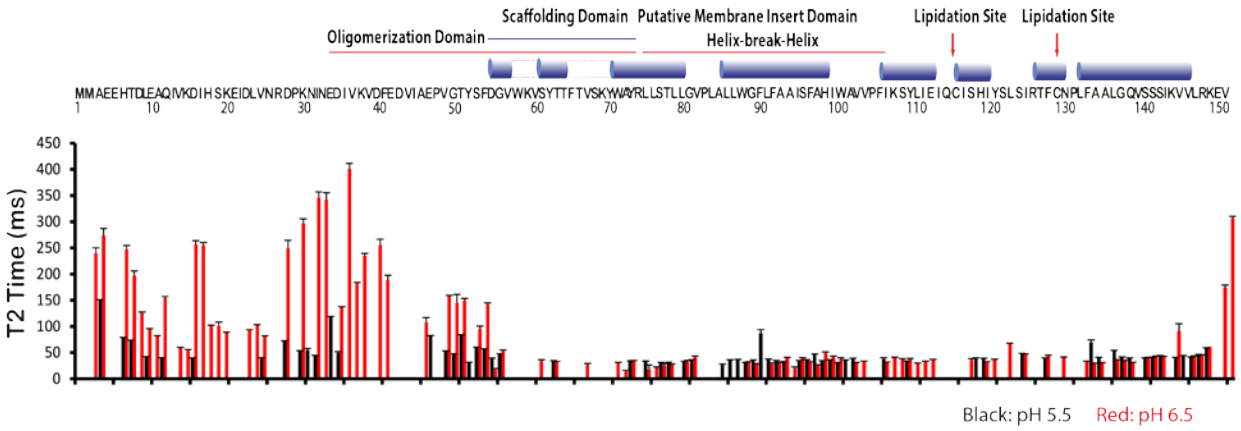

Figure S3. Influence of pH on the dynamics of lipidated Cav3 in LPPG micelles. Backbone transverse relaxation times (T2) of lipidated Cav3 in LPPG micelles at pH 5.5 (black) and 6.5 (red) are plotted against the residue number. T2 of lipidated Cav3 were measured in 5% LPPG micelles at 900 MHz at 45°C. Blank region indicates residues for which peaks could not be assigned. T2 values within the N-terminal domain (residues 3-40) are generally greater at pH 6.5 (red) than at pH 5.5 (black). Error bars for T2 values reflect the uncertainties associated with the fitting of relaxation data.

Figure S4
Kim et al.

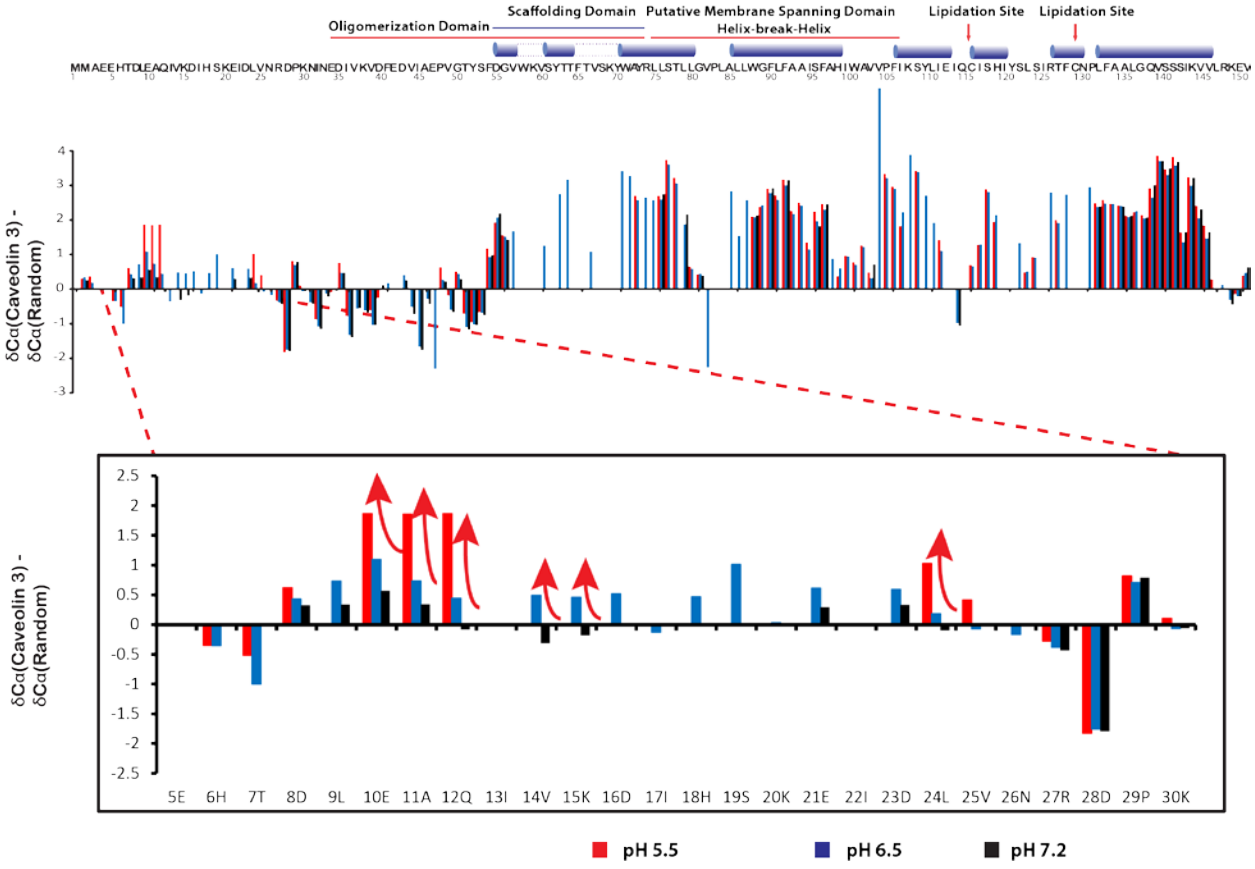

Figure S4. Change in the secondary structure of lipidated Cav3 at low pH in LPPG micelles. Secondary structure predictions based on Chemical Shift Index (CSI) are compared for lipidated Cav3 at pH 5.5 (red), 6.5 (blue), and 7.2 (black). The differences between the observed ^{13}C chemical shifts and standard residue-specific random coil ^{13}C shift values for the backbone carbons (ΔC) are plotted against the residue number at each pH (middle). Blank regions indicate residues that could not be confidently assigned. Consecutive positive ΔC values in ^{13}Cα and ^{13}CO are indicative of α helical secondary structure. Though many peaks are missing due to extreme line broadening, increases in the ΔC value at low pH (red arrows) are suggestive with the formation of a helix from residues 10-24 under this condition (bottom).

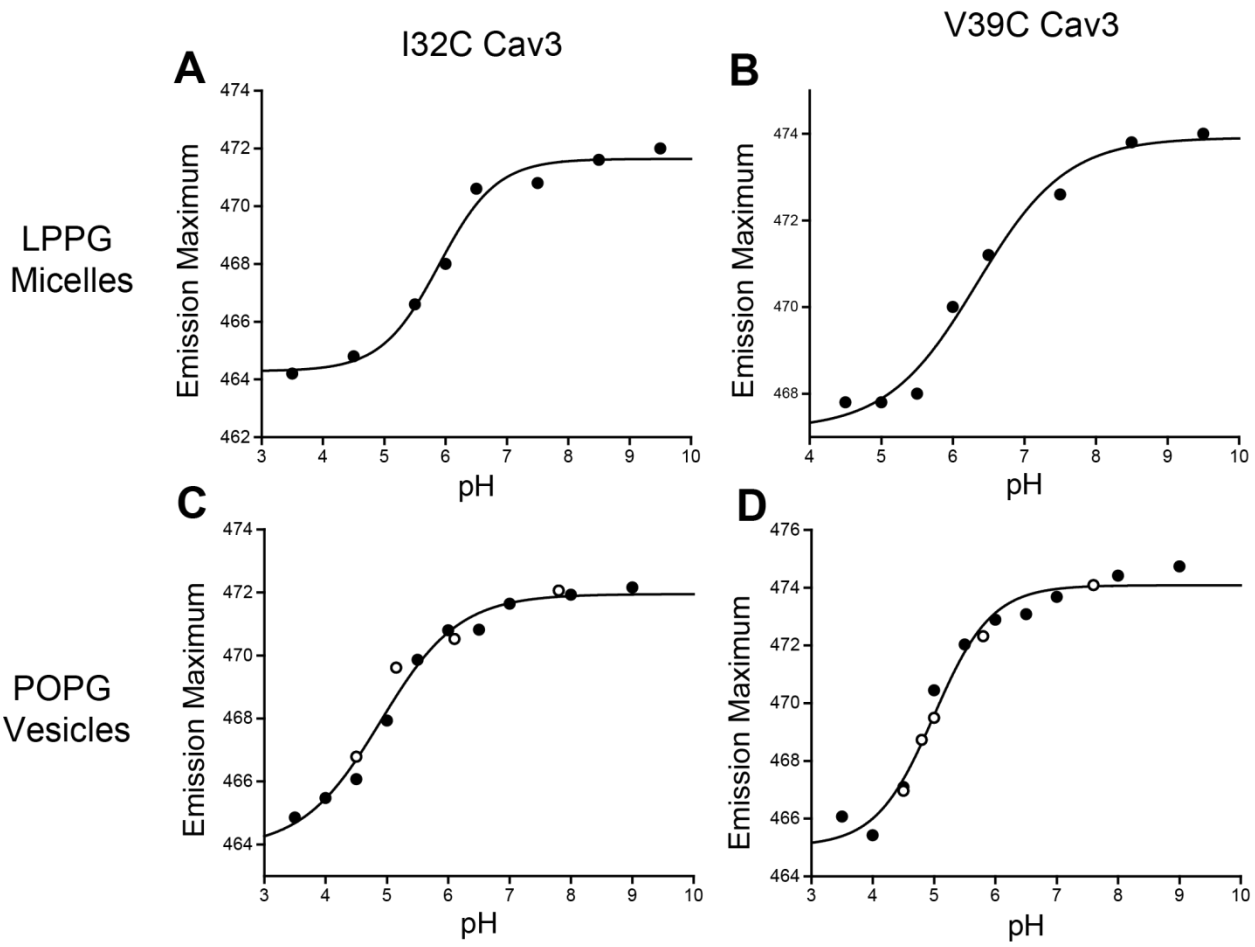

Figure S5. pH-Mediated Conformational Transition in LPPG Micelles and POPG Vesicles. I32C Cav3 (**A** and **C**) and V39C Cav3 (**B** and **D**) were fluorescently labeled with bimane and reconstituted in either 0.1 % (w/v) LPPG micelles (**A** and **B**) or POPG vesicles (250:1 molar lipid: protein), **C** and **D**) in 15 mM acetic acid, 15 mM MES, 30 mM Tris, 120 mM NaCl, and 0.5 mM EDTA with varying pH prior to equilibration at 25 °C. The fluorescence emission spectrum was then collected under each condition, and the emission maximum is plotted against the corresponding pH. Closed circles reflect data for the titration from low pH to high pH. Open circles reflect the data for the titration from high pH to low pH. The data were fit with a model derived from the Henderson-Hasselbalch equation (black line). The apparent pKa values of the transition for I32C Cav3 in LPPG micelles and POPG vesicles were determined to be 5.9 ± 0.1 and 4.9 ± 0.2, respectively. The apparent pKa values of the transition for V39C Cav3 in LPPG micelles and POPG vesicles were determined to be 6.3 ± 0.2 and 5.1 ± 0.1, respectively.

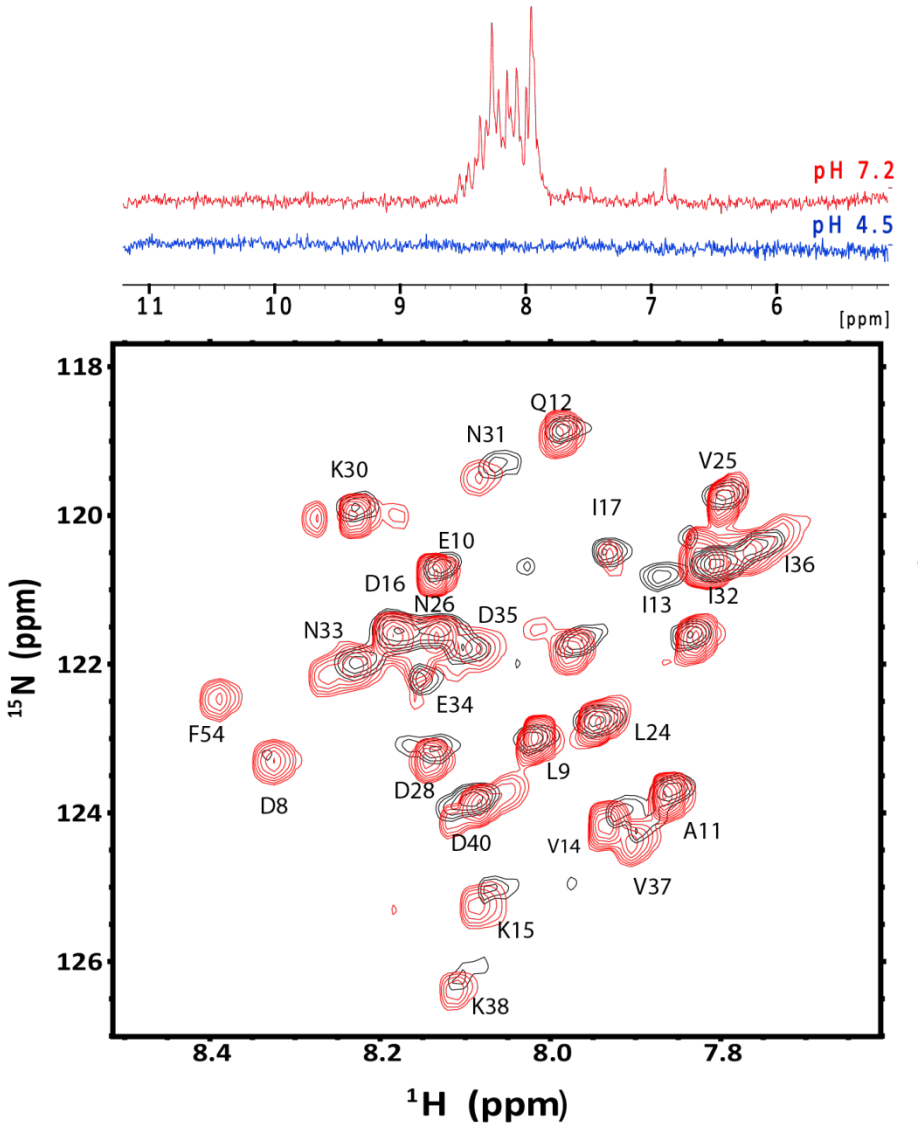

Figure S6. Moving the His_6 tag from the N-terminus to the C-terminus of Cav3 does not alter the pH-dependent topological switch associated with the C-terminal domain: influence of pH on the solution NMR spectra of C-terminally His_6 tagged Cav3. The 1D proton spectrum of C-terminally tagged, lipidated Cav3 in POPG is shown at pH 7.2 (red) and at pH 5.5 (blue). 1D proton spectra of lipidated Cav3 at pH 7.2 (red) and pH 4.5 (blue) in 75 mM imidazole containing 25 mM sodium acetate and 0.5 mM EDTA is shown at the top. Below, the 2D TROSY-HSQC spectrum of C-terminally His_6-tagged, lipidated Cav3 (red) is overlaid on that of the N-terminally tagged, lipidated Cav3 in POPG at pH 7.2 (black). The spectral similarities of these constructs suggest association of the N-terminal domain with the membrane does not arise as a result of the N-terminal poly-histidine tag.

Figure S7
Kim et al.

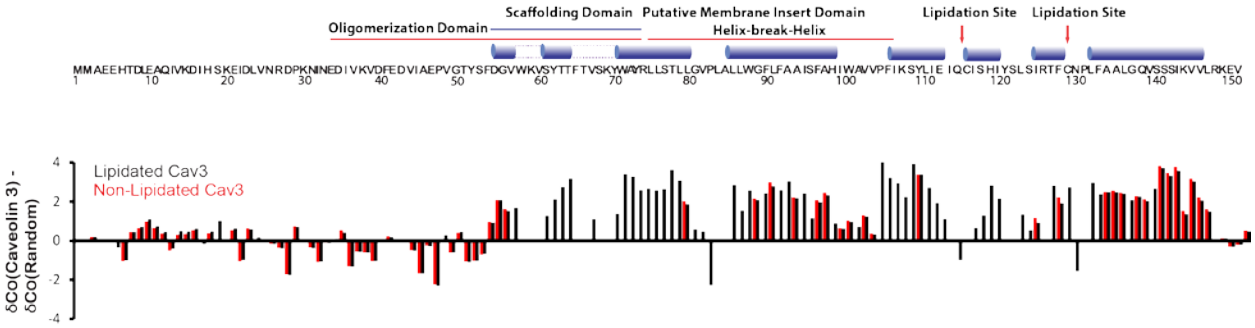

Figure S7. Differences in the secondary structure of lipidated and non-lipidated Cav3 in LPPG micelles at pH 6.5. Secondary structure based on Chemical Shift Index (CSI) are shown for lipidated (black) and non-lipidated (red) Cav3. The differences between the observed ^{13}C chemical shifts and standard residue-specific random coil ^{13}C shift values for the backbone carbons (ΔC) are plotted against the residue number. According to CSI analysis consecutive positive ΔC values in ^{13}CO are indicative of α helical secondary structure. Prominent negative peaks proximal to the modification sites in the lipidated protein suggest the modifications induce helical breaks at these positions.